GENERALIZED PREDICTIVE SPEED CONTROLLER OF DOUBLE STATOR INDUCTION MOTOR

HOUARI. KHOUIDMI AHMED. MASSOUM

Hassiba Benbouali University of Chlef-Algeria
houarikhouidmi@yahoo.fr ahmassoum@yahoo.fr

ABDELKADER. MEROUFEL MELIANI. BOUZIANE

Djillali Liabès University of Sidi Bel-Abbès-Algeria
ameroufel@yahoo.fr melfat06@yahoo.fr

***Abstract*:** *In this paper, a generalized predictive control (GPC) application to double stator induction motor is introduced. First, a model of DSIM is built to describe the prediction model of the process and then the GPC control law is derived and used to design the speed controller. It output is the future value of the controlled variables which is needed by field oriented control procedure (FOC).*

The applications of this strategy in the field of driving machines have been successful for high performance applications, with small overshoot, cancellation of disturbances, good stability and robustness. After analyzing the control strategy, we have shown that it is possible to synthesize a speed control of a double stator induction motor based on a minimal structure using only a simplified model (input-output transfer) and combining in a judicial way the vector control for the decoupling and the generalized predictive control for adjusting the speed. Comparison with results obtained with a more "classical" proportional-integral- (PI) controller is finally given. Therefore, we believe that this work is a contribution to the domain of variable speed multiphase induction motor drive.

***Keywords*:** *Modeling, Double Stator Induction Machine (DSIM), Multilevel Voltage Source Inverter (VSI), Space Vector Pulse Width Modulation (SVPWM), Field Oriented Control (FOC), Generalized Predictive Control (GPC).*

1. INTRODUCTION

The fast progress in the development of ac motor drives in the past two decades was mainly due to the development of power electronic devices [1], powerful and inexpensive microprocessors and modern ac motor technologies. This modern ac motor which has been developed recently is the use of multiphase drives where the number of stator phases is more than three [2, 3, 4]. All evaluations conducted on multiphase drives lead to encouraging results in terms of decrease the single switches current stress instead of adopting parallel techniques, reduce the harmonics content of the DC link current, improve the overall system reliability and correcting the torque ripple [5].

Many scholars have studied multiphase drives with dual stator three-phase motors. Of course, the torque ripple increases with the number of faulty phases because more statorique phase, less disturbance on the torque is important but the results of these research show that the torque ripple is superior to that of normal three-phase motors, in order to reduce this distortion, a variety of approaches in inverter control strategy and speed controller through multilevel converter design and predictive control algorithm [6, 7].

The predictive control aims to obtain certain desired performances in the presence of disturbances and the internal variations, the generalized predictive control constitutes one of the new most interesting solutions to implant during this last decade, in a general way these techniques of predictive controls generated a great number of application in various practical fields [7].

2. MACHINE MODELING

This typical six-phase induction machine can be used in generator systems [8, 9, 10] and in sensorless speed control at low speeds [11, 12], this induction machine has two sets of three-phase windings which are spatially phase shifted by 30 electrical degrees with isolated neutrals. The dual stator three-phase induction machine is a six dimensional system. The original six dimensional machine system can be

decomposed into two-dimensional orthogonal subspaces dq or (α,β)-axis.

The model of the DSIM drive will be described in stator field coordinates. This system of equations is nonlinear. The indices "r", "s1" and "s2" mean rotor, stator1 and stator2 respectively. The Park model in set of equation of state is presented below [13, 14].

$$\frac{d}{dt}[\Phi]=[A][\Phi]+[B][V] \tag{1}$$

Where: $$[\Phi]=\begin{bmatrix}\Phi_{dqs1}\\ \Phi_{dqs2}\\ \Phi_{dqr}\end{bmatrix},[V]=\begin{bmatrix}V_{dqs1}\\ V_{dqs2}\\ V_{dqr}\end{bmatrix} \tag{2}$$

The state matrix A and vector B in the d-q axis are:

$$[A]=\begin{bmatrix}a_{11} & a_{12} & a_{13} & 0 & a_{15} & 0\\ a_{21} & a_{22} & 0 & a_{24} & a_{25} & 0\\ a_{31} & 0 & a_{33} & a_{34} & 0 & a_{36}\\ 0 & a_{42} & a_{43} & a_{44} & 0 & a_{46}\\ a_{51} & a_{52} & 0 & 0 & a_{55} & a_{56}\\ 0 & 0 & a_{63} & a_{64} & a_{65} & a_{66}\end{bmatrix} \tag{3}$$

$$[B]=\begin{bmatrix}1 & 0 & 0 & 0\\ 0 & 1 & 0 & 0\\ 0 & 0 & 1 & 0\\ 0 & 0 & 0 & 1\\ 0 & 0 & 0 & 0\\ 0 & 0 & 0 & 0\end{bmatrix} \tag{4}$$

Where:

$$a_{11}=a_{33}=\frac{L_a}{T_{s1}L_{s1}}-\frac{1}{T_{s1}}$$

$$a_{12}=a_{24}=-a_{31}=-a_{42}=\omega_s, a_{15}=a_{35}=\frac{L_a}{T_{s1}L_r}$$

$$a_{21}=a_{43}=\frac{L_a}{T_{s2}L_{s1}}, a_{22}=a_{44}=\frac{L_a}{T_{s2}L_{s2}}-\frac{1}{T_{s2}}$$

$$a_{25}=a_{46}=\frac{L_a}{T_{s2}L_r}, a_{51}=a_{63}=\frac{L_a}{T_{s1}L_r}$$

$$a_{52}=a_{64}=\frac{L_a}{T_{s2}L_r}, a_{55}=a_{66}=\frac{L_a}{T_rL_r}-\frac{1}{T_r}$$

$$a_{56}=-a_{65}=\omega_r, T_s=\frac{L_s}{R_s}, T_r=\frac{L_r}{R_r}$$

The mechanical equation is:

$$J\frac{d\Omega_m}{dt}=T_e-T_m-K_f.\Omega_m \tag{5}$$

The equation of the electromagnetic torque is:

$$T_e=p\frac{L_m}{L_m+L_r}\left[(I_{qs1}+I_{qs2}).\Phi_{dr}-(I_{ds1}+I_{ds2}).\Phi_{qr}\right] \tag{6}$$

3. SUPPLY SYSTEM MODELING

The structure of a typical five-level voltage source inverter (VSI) of diode-clamped that uses IGBT devices is shown in fig.1. The higher number of levels provides the advantages of higher power rating and lower output harmonics [15, 16].

A five-level inverter has 5^3= 125 switching states, 8 switching devices and 6 clamping diodes for each phase leg, and 4 DC- side capacitors, where each switching device shares $V_{dc}/4$ voltage [1]. It produces 5 level phase voltage, 9 level line voltage waves, 61 voltage space vectors. (See fig.2)

Table 1 shows the device switching table for a phase group and the corresponding phase voltage level or state, e.g. state 1 corresponds to output voltage 0.25 V_{dc} and the switching group is closed such that positive current can flow through S4, S5 and S6, and negative current flow through S7.

Figure 3 shows what the space vector d-q plane looks like for a five-level inverter [17, 18]. Each vector on the space vector plane represents a particular three-phase output voltage state of the inverter. For example, the vector V^{210} on the space vector plane means; that with respect to ground, a phase is at $2V_{dc}$, b phase is at $1V_{dc}$, and c phase is at $0V_{dc}$. For an output voltage state V^{xyz} in five-level diode-clamped inverter, the number of redundant states available is given by 5 – 1 – max(x, y, z). Switch state (2, 1, 0) has redundant states (3, 2, 1) and (4, 3, 2). Redundant switching states differ from each other by an identical integral value, i.e., (2, 1, 0) differs from (3, 2, 1) by (0, 0, 0) and from (4, 3, 2) by (1, 1, 1). The number of distinct or unique switching states is 5^3-$(5\text{-}1)^3$=61. Therefore, the number of redundant switching states is 4^3=64. The number of possible zero states is equal to the number of levels; for a five-level diode-clamped inverter, the zero voltage states are V^{000}, V^{111}, V^{222}, V^{333} and V^{444} [18]. Table 2 summarizes the available redundancies and distinct states for a five-level diode-clamped inverter.

Table 1
Switching states of a phase group for a five level inverter

Switching states	S1	S2	S3	S4	S5	S6	S7	S8	V_N
4	on	on	on	on	off	off	off	off	V_{dc}
3	off	on	on	on	on	off	off	off	$3V_{dc}/4$
2	off	off	on	on	on	on	off	off	$V_{dc}/2$
1	off	off	off	on	on	on	on	off	$V_{dc}/4$
0	off	off	off	off	on	on	on	on	0

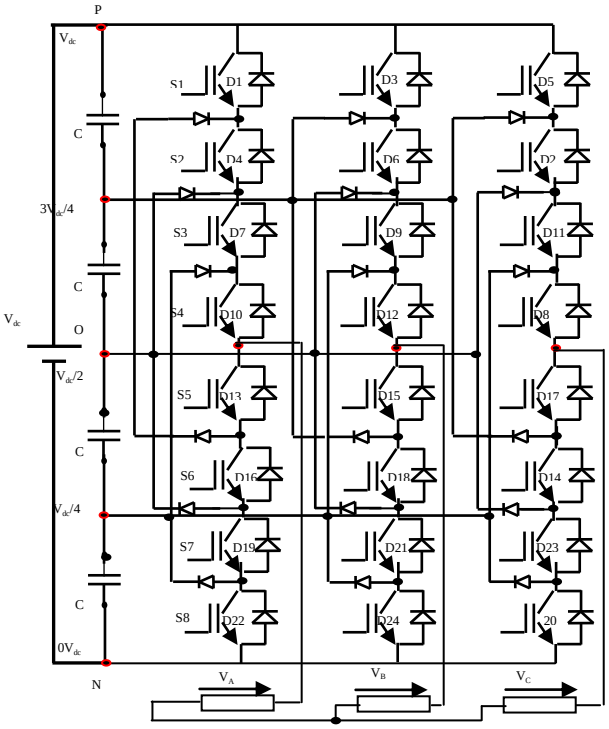

Fig.1. Five-level diode clamped inverter

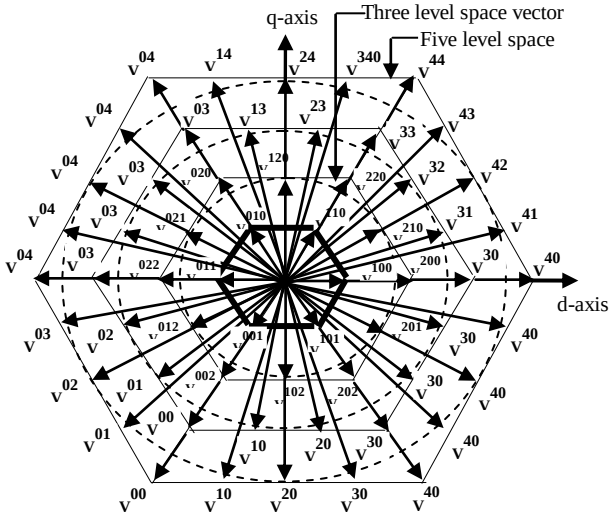

Fig.2. Space vector of multi-level inverter

The output voltages are:

$$V_{abcN} = M_{abc}.V_c \quad (7)$$

Where: $V_c=[V_{c1}\ V_{c2}\ V_{c3}\ V_{c4}]^T$;

$$M_{abcN} = \left[\sum_{i=0}^{4} \delta(S_{abc} - i)\right] \text{ and } V_{abcN} = \begin{bmatrix} V_{aN} \\ V_{bN} \\ V_{cN} \end{bmatrix}$$

Where S_{abc} is the switch state of phases a, b and c respectively; and i is an integer from 1 to 4.

Where $\delta(S_{abc}\text{-}i) = 1$ if $S_{abc}\text{-}i \geq 0$,

$\delta(S_{abc}\text{-}i) = 0$ if $S_{abc}\text{-}i < 0$.

As an example, for the space vector V^{210}; $S_a = 2$,

$S_b = 1$, $S_c = 0$, the M_{abcN} matrix for this particular switching state of a five-level inverter would be:

$$M_{abcN} = \begin{bmatrix} 1 & 1 & 0 & 0 \\ 1 & 0 & 0 & 0 \\ 0 & 0 & 0 & 0 \end{bmatrix}$$

Table 2
Line-line redundancies of five-level three-phase diode clamped inverter.

Redundancies	**Distinct States**	**Redundant States**	**Unique State Coordinates: (a, b, c) where 0≤ a,b,c ≤4**
4	1	4	(0,0,0)
3	6	18	(0,0,1),(0,1,0), (1,0,0),(1,0,1), (1,1,0),(0,0,1)
2	12	24	(p,0,2),(p,2,0), (0,p,2),(2,p,0), (0,2,p,),(2,0,p) where p≤2
1	18	18	(0,3,p),(3,0,p), (p,3,0),(p,0,3), (3,p,0),(0,p,3) where p≤3
0	24	0	(0,4,p),(4,0,p), (p,4,0),(p,0,4), (4,p,0),(0,p,4) where p≤4
Total	61	64	Total=61+64= $125=5^3$ stats

4. FIELD ORIENTED CONTROL OF DSIM

The goal of this method is to make the DSIM motor emulate the dc motor control by transforming the stator currents to a specific coordinate system where one coordinate is related to the torque production and the other to the rotor flux [19, 20], by eliminating the rotor currents, equations (8) and (9) can be derived relating rotor fluxes with stator currents. Substituting the conditions $\Phi_{qr} = 0$ and $\frac{d\Phi_{qr}}{dt} = 0$ for decoupled control and $\frac{d\Phi_{dr}}{dt} = 0$ for constant flux, equations (10) and (11) can be derived. Equation (10) indicates how the control slip command ω_g^* can be derived in feed-forward manner

from the control currents I_{qs1} and I_{qs2}, whereas equation (11) shows that rotor flux is a function of I_{ds1} and I_{ds2} in the steady-state condition.

$$\frac{d\Phi^*_{dr}}{dt} + \frac{R_r}{L_r}(\Phi^*_{dr} - \Phi^*_{dm}) - \omega^*_g \Phi^*_{qr} = 0 \quad (8)$$

$$\frac{d\Phi^*_{qr}}{dt} + \frac{R_r}{L_r}(\Phi^*_{qr} - \Phi^*_{qm}) - \omega^*_g \Phi^*_{dr} = 0 \quad (9)$$

$$\omega^*_g = \omega^*_r = \omega^*_s - \omega_m = \frac{R_r}{L_m + L_r}(I^*_{qs1} + I^*_{qs2}) \quad (10)$$

$$\Phi_r = \Phi^*_{dr} = L_m(I_{ds1} + I_{ds2}) \quad (11)$$

Where: $\omega_m = p.\Omega_m$

FOC needs two constant input references the torque component and the flux component [4, 12], by maintaining the amplitude of the rotor flux (Φ_r) at a fixed value we have a linear relationship between torque and flux:

$$T^*_{em} = p\frac{L_m}{L_m + L_r}(I_{qs1} + I_{qs2}).\Phi^*_{dr} \quad (12)$$

The relations between voltages and currents components are:

$$\begin{aligned}
V^*_{ds1} &= R_{s1}I_{ds1} + pL_{s1}I_{ds1} - \omega^*_s(L_{s1}I_{qs1} + T_r\Phi^*_{dr}\omega^*_g)\\
V^*_{qs1} &= R_{s1}I_{qs1} + pL_{s1}I_{qs1} + \omega^*_s(L_{s1}I_{ds1} + \Phi^*_{dr})\\
V^*_{ds2} &= R_{s2}I_{ds2} + pL_{s2}I_{ds2} - \omega^*_s(L_{s2}I_{qs2} + T_r\Phi^*_{dr}\omega^*_g)\\
V^*_{qs2} &= R_{s2}I_{qs2} + pL_{s2}I_{qs2} + \omega^*_s(L_{s2}I_{ds2} + \Phi^*_{dr})
\end{aligned} \quad (13)$$

For a perfect decoupling we will add new currents regulators [15, 20], command I^*_{dqs1} generated by Φ^*_{dr} (constant or programmed with speed for field-weakening control) is compared with the corresponding machine value, which then generates V^*_{dqs1} and V^*_{dqs2} command after adding the decoupling compensation voltages V_{dqs1c} and V_{dqs2c} in the control loop.

$$\begin{aligned}
V^*_{ds1} &= V_{ds1} - V_{ds1c}\\
V^*_{qs1} &= V_{qs1} + V_{qs1c}\\
V^*_{ds2} &= V_{ds2} - V_{ds2c}\\
V^*_{qs2} &= V_{qs2} + V_{qs2c}
\end{aligned} \quad (14)$$

Where:

$$\begin{aligned}
V_{ds1c} &= \omega^*_s(L_{s1}I_{qs1} + T_r\Phi_r\omega^*_g)\\
V_{qs1c} &= \omega^*_s(L_{s1}I_{ds1} + \Phi_r)\\
V_{ds2c} &= \omega^*_s(L_{s2}I_{qs2} + T_r\Phi_r\omega^*_g)\\
V_{qs2c} &= \omega^*_s(L_{s2}I_{ds2} + \Phi_r)
\end{aligned} \quad (15)$$

In indirect vector control (IVC), the slip command signal ω^*_g is derived from the command I_{qs1} through the slip gain $\frac{2L_m}{T_r}$. This signal is then added to the speed signal ω_m, and then the slip ω^*_s command is derived. In the constant torque region, the rated flux is generated by constant I_{ds1} command. For closed-loop flux control in both constant-torque and field-weakening regions, I_{ds1} can be controlled within the programmed flux control loop so that the inverter always operates in SVPWM mode. The loss of flux in the field-weakening region causes some loss of torque from that of the square-wave mode, but fast vector control response is retained.

5. GENERALIZED PREDICTIVE CONTROL

This part reviews the main developments in generalized predictive control (GPC) [7, 21, 22].

The predictive strategy can be summarized by the following points:

1 - Predict each time, the output on a finite horizon, and that using a numerical model of the system.

2 - Develop a sequence of future control by minimizing a quadratic criterion on the future errors between the output and the trajectory to be followed, with a weight on the command.

3- Implement a strategy based on the principle of receding horizon.

A. PREDICTION MODEL

The numerical prediction model is classically defined by input/output transfer function. The model is represented as CARIMA (Controlled Auto-Regressive Integrated Moving Average) by fixing the polynomial 'noise' $C(q^{-1}) = 1$:

$$A(q^{-1})\Omega(k) = B(q^{-1})T_{em}(k-d) + \xi(k)/\Delta(q^{-1}) \quad (16)$$

$\Delta(q^{-1}) = 1 - q^{-1}$, $T_{em}(k)$ and $\Omega(k)$ are respectively the input and output of the model, $\xi(k)$ is a centered white noise, q^{-1} is the delay operator, d is the delay

introduced by the system and $A(q^{-1})$ and $B(q^{-1})$ are two polynomials defined by:

$$\begin{cases} A(q^{-1}) = 1 + a_1 q^{-1} + \ldots\ldots + a_{n_a} q^{-n_a} \\ B(q^{-1}) = b_0 + b_1 q^{-1} + \ldots\ldots + b_{n_b} q^{-n_b} \end{cases} \quad (17)$$

The introduction of the difference operator $\Delta(q^{-1})$ in the disturbance model helps to find an integral action in the controller and so eliminate static errors [21].

B. MATRIX OPTIMAL PREDICTOR

In this section, we calculate Ω(k+j), the prediction at time k of Ω at j sampling step ahead. This calculation requires the solution of two Diophantine equations, based on the model mentioned in (16) and applying the ideas of modeling presented by Clarke and his co-authors [7], the predicted output Ω(k+j) is decomposed in a conventional manner in response free and forced, including a polynomial form to complete the synthesis polynomial final, single solution of Diophantine equations:

$$\begin{aligned} \Omega(k+d+j) &= F_j(q^{-1})\Omega(k) + H_j(q^{-1})\,\Delta T_{em}(k-1) + \\ &+ G_j(q^{-1})\,\Delta T_{em}(k+j-1) + J_j(q^{-1})\,\xi(k+d+j) \end{aligned} \quad (18)$$

With: F_j, G_j, H_j, J_j polynomials single solutions of the following Diophantine equations:

$$\begin{aligned} &\Delta(q^{-1})A(q^{-1})J_j(q^{-1}) + q^{-d-j}F_j(q^{-1}) = 1 \\ &G_j(q^{-1}).(1) + q^{-j}H_j(q^{-1}) = B(q^{-1})J_j(q^{-1}) \end{aligned} \quad (19)$$

The optimal predictor is then defined by considering that the best prediction of noise in the future is its medium (supposed zero here), either:

$$\begin{aligned} \hat{\Omega}(k+j) &= F_j(q^{-1})\Omega(k) + H_j(q^{-1})\Delta T_{em}(k-1) + \\ &+ G_j(q^{-1})\Delta T_{em}(k+j-1) \end{aligned} \quad (20)$$

With: $\text{degree } J_j(q^{-1}) = \text{degree } G_j(q^{-1}) = j - d$

$\text{degree } F_j(q^{-1}) = \text{degree } A(q^{-1})$

$\text{degree } H_j(q^{-1}) = \text{degree}[B(q^{-1})] - 1$

To simplify the notations, it is possible to use a matrix representation of this predictor. Let us pose for that:

$$\Psi = [\Psi(k+d+N_1) \ldots\ldots \Psi(k+d+N_2)]^T \quad (21)$$

$$f(q^{-1}) = [F_{N_1}(q^{-1}) \ldots\ldots\ldots F_{N_2}(q^{-1})]^T \quad (22)$$

$$h(q^{-1}) = [H_{N_1}(q^{-1}) \ldots\ldots H_{N_2}(q^{-1})]^T \quad (23)$$

$$\tilde{T}_{em} = [\Delta T_{em}(k) \ldots\ldots\ldots\ldots \Delta T_{em}(k+N_u-1)]^T \quad (24)$$

$$G = \begin{bmatrix} g_{N_1}^{N_1} & g_{N_1-1}^{N_1} & \ldots\ldots & \ldots\ldots \\ g_{N_1+1}^{N_1+1} & g_{N_1}^{N_1+1} & \ldots\ldots & \ldots\ldots \\ \ldots\ldots & \ldots\ldots & \ldots\ldots & \ldots\ldots \\ g_{N_2}^{N_2} & g_{N_2-1}^{N_2} & \ldots\ldots & g_{N_2-N_u+1}^{N} \end{bmatrix} \quad (25)$$

With: $\Delta T_{em}(k+j) = 0$ for $j \geq N_u$

The criterion requires the definition of four parameters of adjustment:

N_1: Initialization horizon;

N_2: Prediction horizon;

N_u: Control horizon;

λ: Control weighting coefficient.

With these notations, the optimal predictor with j-step can be written in matrix form:

$$\hat{\Omega} = G\tilde{T}_{em} + f(q^{-1})\Omega(k) + h(q^{-1})\Delta T_{em}(k-1) \quad (26)$$

C. MATRIX COST FUNCTION

The minimization of the criterion is based on the setting in matrix form of the cost function (32):

$$\begin{aligned} J = &\begin{bmatrix} G\tilde{T}_{em} + f\,\Omega(k) + \\ + h\,\Delta T_{em}(k-1) - \Psi \end{bmatrix}^T \\ &\begin{bmatrix} G\tilde{T}_{em} + f\,\Omega(k) + \\ + h\Delta T_{em}(k-1) - \Psi \end{bmatrix} + \lambda\, \tilde{T}_{em}{}^T \tilde{T}_{em} \end{aligned} \quad (27)$$

The optimal control is obtained finally by analytical minimization of the criterion in matrix form, $\frac{\partial J}{\partial \tilde{T}_{em}} = 0$. what leads to the optimal sequence of future control:

$$\tilde{T}_{em} = M[\Psi - f(q^{-1})\Omega(k) - h(q^{-1})\Delta T_{em}(k-1)] \quad (28)$$

With: $M = [G^T G + \lambda I_{N_u}]^{-1} G^T = \begin{bmatrix} m_1^T \\ m_2^T \\ \vdots \\ m_{N_u}^T \end{bmatrix}$ (29)

$$\tilde{T}_{em} = [\,\Delta T_{em}(k)_{opt} \ldots\ldots \Delta T_{em}(k+N_u-1)_{opt}\,]^T \qquad (30)$$

In a traditional way in generalized predictive control, only the first value of the sequence, equation (30) is applied to the system, according to the principle of the receding horizon [23]:

$$\begin{aligned} T_{em}(k) &= T_{em}(k-1) - m_1^T \\ &\quad [\, f(q^{-1})\Omega(k) + h(q^{-1})\Delta T_{em}(k-1) - \Psi\,] \end{aligned} \qquad (31)$$

With: m_1^T first line of the matrix M

6. SIMULATION RESULTS

The double stator three phase induction motor (Fig.3) with the parameters shown in Table 3, is controlled by a cascades type control, the internal loops of torque and flux being conceived around a vector control, the external speed loop including the predictive law. The internal loop east gathers two current loops imposing the currents I_{ds12} and I_{qs12}. The external loop includes the GPC controller (providing the reference torque to the intern loop). Simulations and the tests carried out were focused around this external speed loop.

The construction of the predictive control laws requires the existence of a prediction model of the machine resulting from a step of experimental identification [24]. The electric part is represented by a transfer function of one order. This function thus uses a time-constant: τ_e

$$\frac{T_{em}}{T_{em}^*} = \frac{1}{1+\tau_e s} \qquad (32)$$

s : Variable of Laplace
T_{em} : Electromagnetic torque
T^*_{em}: Reference torque.

The mechanical part of DSIM is characterized by inertia J, the coefficient of viscous friction K_f and the torque load T_r. The time constant τ_e represent the electric part of the DSIM. The relation between the electromechanical torque T_{em} and speed Ω is thus of the form:

$$\left.\begin{aligned} T_{em} &= J\frac{d\Omega}{dt} + k_f\Omega \\ T_{em} &= (Js + k_f)\Omega \end{aligned}\right\} \Rightarrow \frac{\Omega}{T_{em}} = \frac{1}{J.s + k_f} \qquad (33)$$

These elements (electrical and mechanical part) make it possible to build a complete model of the system to be controlled, used during the synthesis of the predictive laws. Figure 4 summarizes this model, showing the mechanics and electric parts as well as the blocker of zero order [25]. Finally, the model used is represented by a discrete transfer function (for one period of sampling of T_s = 101[µs]) between the electromechanical torque and the angular velocity:

$$\frac{\Omega(q^{-1})}{T^*_{em}(q^{-1})} = q^{-1}\frac{B(q^{-1})}{A(q^{-1})} = q^{-1}\,\frac{(0.0774 + 0.07486\ q^{-1})}{1 - 1.905\ q^{-1} + 0.9048\ q^{-2}} \qquad (34)$$

By considering the rules of stability and robustness, a corrector GPC can be synthesized with the set of parameters: N_1 = 1; N_2= 15, N_u = 2 and λ= 53

A five-level inverter has several advantages over a conventional two-level inverter (see fig.5); one particular not only can generate the output torque with very low distortion.

The results of the speed regulation with GPC regulator are shown in figure (6), the corresponding speed and torque of motor tends to its reference command in the proposed control. The speed is linearly increased from zero to 2751[rpm] in 0.9 second without overtaking. After 1.5 seconds, a nominal load torque of 14 [N.m] is applied to appreciate the dynamic response of the DSIM.

Fig.7 shows the simulation results of the speed reversal test, in this test the DSIM runs with positive nominal speed, and then the speed is reversed linearly in 2 sec. The amplitude of rotor flux is kept constant on 1[Wb]. These results verify the ability of IFOC during speed reversal. It is evident that the flux of the DSIM remains unaffected during the transient of the speed.

Fig.8 shows the simulation results of the robustness test, in this test the DSIM runs with positive unmeasured disturbance of 7 [N.m], these results verify the ability of GPC controller during load change. We remark that the GPC and PI response time control are evaluated at 1 sec and 1.2 sec respectively. The GPC overshoot is evaluated at 3%, these PI overshoot is equal to 9%.

One notes according to the simulation results that the variations of the real and reference speed present a similar dynamic in terms of continuation and establishment. This dynamic is sensitive for the inverter levels and modulation strategy.

8. CONCLUSION

In this paper, we might focus the GPC performances of DSIM by using GPC controller for mechanical speed adjustment. The proposed strategy was applied to a double stator induction motor operating under FOC technique.

The obtained simulation results show a clear improvement on the level of the machine response by using the simplified model of the machine. High robustness with respect to the unmeasured disturbance load is checked during simulation compared to the traditional control.

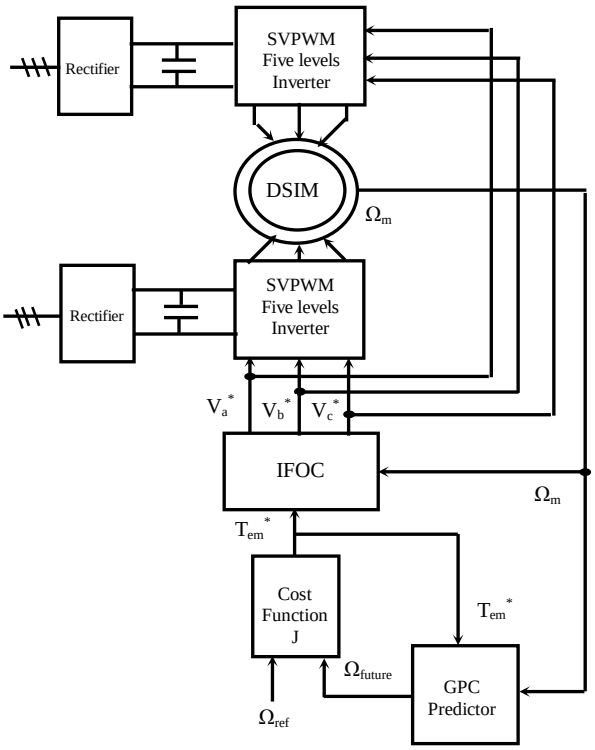

Fig.3. Cascade Control of DSIM

Table 3
Double Stator Induction Motor Parameters

Nominal values	Value	IS-Unit
Power	4.5	kW
Frequency	50	Hz
Voltage (Δ/Y)	220/380	V
Current (Δ/Y)	5.6	A
Speed	2751	rpm
Poles of pair	1	
$Rs_1 = Rs_2$	3.72	Ω
Rr	2.12	Ω
$Ls_1 = Ls_2$	0.022	H
Lr	0.006	H
L_m	0.3672	H
J	0.0625	Kgm^2
K_f	0.001	$Nm(rad/s)^{-1}$

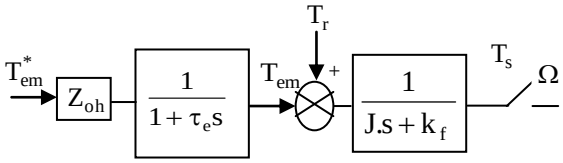

Fig.4. Simplified model of the control law

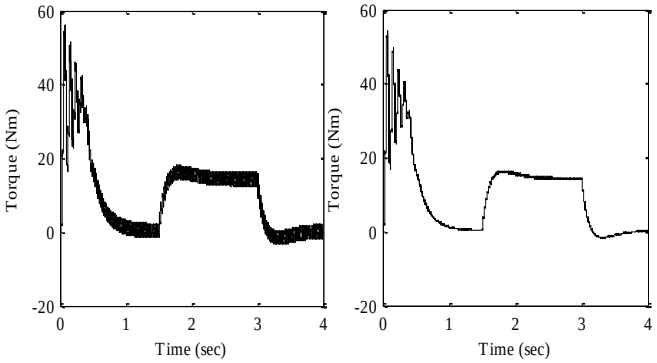

(a) Two-level VSI (b) Five-level VSI

Fig.5. The electromagnetic torque

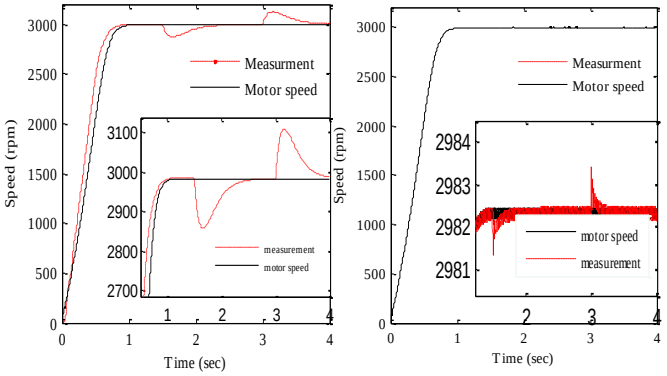

(a) PI regulator (b) GPC regulator

Fig.6. The mechanical speed

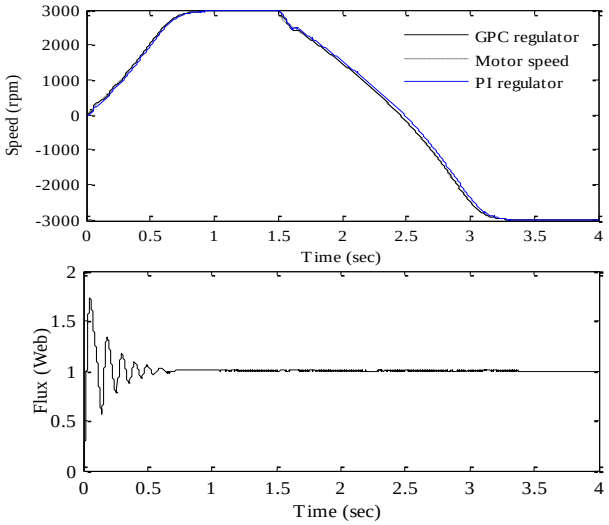

Fig.7. The inversion speed test

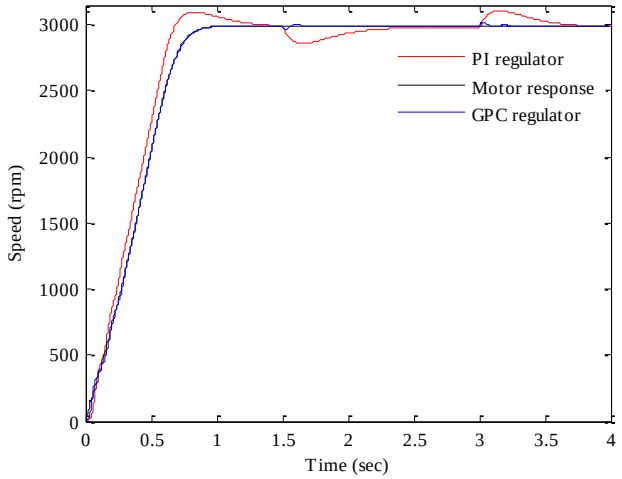

Fig.8. The robustness test (unmeasured disturbance)

REFERENCES

[1] Bose,B.K, "*Modern Power Electronics and AC Drives*", University of Tennessee. Prentice Hall PTR, New Jersey, 2002.

[2] G. K. Singh, "*Multi-Phase Induction Machine Drive*" Research-A Survey, Elect. Power Syst. Res **62 (**2002**)** 139–147.

[3] E. A. Klingshirn, "*High Phase Order Induction Motors-Part II Experimental Results*", IEEE Trans. Power App. Syst. **102 (**1983**)** 54–59.

[4] G. K. Singh, K. Nam, S. K. Lim, "*A Simple Indirect Field-Oriented Control Scheme for Multiphase Induction Machine*", IEEE Trans. Ind Appl **52** (2005) 1177–1184.

[5] R. O. C. Lyra and T. A. Lipo, "*Torque density improvement in a six-phase induction motor with third harmonic current injection*", IEEE Trans. Ind Appl **38** (2001) 1779–1786.

[6] L. M. Tolbert, F. Z. Peng, and T. Habetler, "*Multilevel Converters for Large Electric Drives*", IEEE Trans. Ind Appl **35** (1999) 36– 44.

[7] D.W. Clarke, C. Mohtadi, P.S. Tuffs, "*Generalized predictive control*" – parts 1 and 2, Automatica **23** (1987) 137–160.

[8] L. Xu and L. Ye, "*Analysis of a novel stator winding structure minimizing harmonic current and torque ripple for dual six-step converter-fed high power AC machines*", IEEE Trans. Ind Appl **31 (**1995**)** 84– 90.

[9] P. L. Alger, E. H. Freiburghouse, and D. D. Chase, "*Double windings for turbine alternators*", AIEE Trans **49** (1930) 226 –244.

[10] R. Schiferl, "*Detailed analysis of a six phase synchronous machine with AC and DC stator connections*", Ph.D. dissertation, Elect. Eng. Dep, Purdue Univ, West Lafayette, IN, 1982.

[11] M. Shin, D. Hyun, S. Cho, and S. Choe, "*An improved stator flux estimation for speed sensorless stator flux orientation control of induction motors*", IEEE Trans. Power Electron **15** (2000) 312–318.

[12] G. R. Arab Markadeh, J. Soltani, N. R. Abjadi, M. Hajian, "*Sensorless Control of a Six-Phase Induction Motors Drive Using FOC in Stator Flux Reference Frame*", World Academy of Science, Engineering and Technology **58** (2009) 553–559.

[13] D. Hadiouche, "*Contribution to the study of dual stator induction machines: modelling, supplying and structure*", Ph. D. dissertation (in French), GREEN, Faculty of Sciences and Techniques, University Henri Poincaré-Nancy I, France, 2001.

[14] Alfredo R. Muñoz, and Thomas A. Lipo, "*Dual Stator Winding Induction Machine Drive*", IEEE Trans. Ind Appl **36** (2000) 1369–1379.

[15] B. K. Bose, "*Power Electronics and Motor Drives*", Elsevier/Academic Press, 2006.

[16] R.W. Menzies, P. Steimer, J.K. Steinke, "*Five-level GTO inverters for large induction motor drives*", IEEE Trans. Ind Appl **30** (1994) 938– 944.

[17] H.W. Van Der Broeck, H.C. Skudelny, G.V. Stanke, "*Analysis and Realization of a pulse width modulation based on voltage space vectors*", IEEE Trans. Ind Appl **24** (1988) 142–150.

[18] Y. Zhao and T. A. Lipo, "*Space Vector PWM Control of Dual Three phase Induction Machine Using Vector Space Decomposition*", IEEE Trans. Ind Appl **31** (1995) 1100–1109.

[19] R. Bojoi, M. Lazzari, F. Profumo and A. Tenconi, "*Digital Field-Oriented Control for Dual Three-Phase Induction Motor Drives*", IEEE Trans. Ind Appl **39** (2003) 752–760.

[20] D. Lee, S. Ki Sul, M. Park, "*High Performance Current Regulator For a Field-Oriented Controlled Induction Machine Drive*", IEEE Trans. Ind Appl **30**, (1994) 1247– 1257.

[21] J. Richalet, A. Rault, J.L. Testud and J. Papon, "*Model Predictive Heuristic Control: applications to industrial processes*", Automatica, **14** (1978) 413–428.

[22] T. Gallah, A. Khedher, M. F. Mimouni and F. M'sahli, "*Theoretical comparison between Field Oriented and Generalized Predictive Control for an Induction Motor*", Int. Journal on Sciences and Techniques of Automatic control **1** (2007) 43–60.

[23] W.H. Kwon and S. Han, "*Receding Horizon Control*", Springer Press, UK, 2005.

[24] L. Ljung: "*System Identification*", Theory for the User, 2nd Edition, PTR Prentice Hall, New Jersey, 1999.

[25] T. Soderstrom, P. Stoica, "*System Identification*", Prentice Hall International, New York, 1989.